J. Amer. Soc. Hort. Sci. 149(3):121–130. 2024. https://doi.org/10.21273/JASHS05378-24

# Analysis of Microstructure, Cell Wall Polysaccharides, and Candidate Cell Wall-related Genes in Clingstone-type and Freestone-type Stony Hard Peaches during Ripening

**Hongmei Wang, Ang Li, Wenyi Duan, Junren Meng, Yule Miao, Zhenyu Yao, Akhi Badrunnesa, Liang Niu, Lei Pan, Guochao Cui, Shihang Sun, Zhiqiang Wang, and Wenfang Zeng**

*Zhengzhou Fruit Research Institute, Chinese Academy of Agricultural Sciences, Zhengzhou, Henan 450009, China; and Zhongyuan Research Center, Chinese Academy of Agricultural Sciences, Xinxiang, Henan 453000, China*

**Guohuai Li**

*Huazhong Agricultural University, Wuhan, Hubei 430070, China*

**Keywords.** cellulose, firmness, mealiness, pectin, *Prunus persica*

**Abstract. Stony hard (SH) peach (*Prunus persica*) fruits produce no ethylene and clingstone-type SH peaches have a crispy flesh texture; however, freestone-type SH peach fruits ripen to a soft, mealy state. During this study, we compared and analyzed changes in the microstructure, cell wall polysaccharides, and candidate cell wall-related genes of freestone-type SH 'Zhongtao 14' ('CP14'), 'Zhongtao White Jade 2' ('CPWJ2'), clingstone-type SH 'Zhongtao 13' ('CP13'), and 'Zhongtao 9' ('CP9') during fruit ripening. The parenchyma cells of mealy freestone-type SH peaches became detached, were single, dried, and irregularly arranged, and remained intact in comparison with the nonmealy clingstone-type SH peaches. Methyl-esterified homogalacturonan was strongly immunolabeled in the cell wall of clingstone SH peaches; however, nonmethylated homogalacturonan was weakly immunolabeled in freestone SH peaches. A transcriptome analysis was performed to investigate the molecular mechanism of the mealiness process. A principal component analysis indicated that 'CP14' S4 III (mealy) could be distinguished from the samples of 'CP13' (S4 I, S4 II, S4 III) and 'CP14' (S4 I, S4 II). The highly coexpressed gene modules linked with firmness were found using a weighted gene coexpression network analysis; 189 upregulated genes and 817 downregulated genes were identified. Six upregulated cell wall-related genes (*PpPG1*, *PpPG2*, *PpAGP1*, *PpAGP2*, *PpEXT1*, and *PpEXP1*) and one downregulated cell wall-related gene (*PpXET2*) were involved in the mealiness process during freestone-type SH fruit ripening. These findings will improve our understanding of the relationship between clingstone, freestone, and stony hard fruits and lay the foundation for further exploration of the mechanisms underlying the softening of peach fruits.**

The softening of fruits during ripening is accompanied by changes in the texture of fruits (Tucker et al. 2017) and is mainly caused by cell wall polysaccharide degradation, pectin solubilization, and cell structure destruction. Peach fruits are classified as melting flesh (MF), nonmelting flesh (NMF) (Lester et al. 1996), and stony hard (SH) (Haji et al. 2005) types based on their firmness. The MF peaches release large amounts of ethylene during ripening and soften rapidly, whereas NMF peaches lack the final melting phase of softening; therefore, they are relatively firm when fully ripe (Brummel et al. 2004b). In contrast to MF and NMF peaches, SH peaches are hard when fully ripe, do not produce large amounts of ethylene during ripening, have a long postharvest shelf life, and are considered to have high breeding value (Liverani et al. 2002; Zeng et al. 2020). It was thought that the SH peach fruits never soften and produce no ethylene. The first selected SH trait ('Jingyu') at the Beijing Forestry and Pomology Institute (Beijing, China) was "practically freestone-NMF" (Sandefur et al. 2013). However, the freestone NMF phenotype has not been reported (Van Der Heyden et al. 1997). The texture of stone adhesion (clingstone/freestone) is simply controlled and inherited by the freestone (Prupe.4G262200) (Gu et al. 2016). It was found that peach chromosome 4 harbors two linked polygalacturonase (PG)-encoding genes, *PGF* (Prupe.4G262200) and *PGM* (Prupe.4G261900), which together control the clingstone/freestone and MF/NMF traits of the fruit (Gu et al. 2016).

The microstructure of the fruit tissue and chemistry changes of the cell wall were closely related to the fruit ripening pattern. Cell-to-cell adhesion affects the fracture path across tissues (Ng et al. 2013). Peach microstructure investigations revealed that parenchyma cells are uniformly and densely packed in the firm

Received for publication 18 Jan 2024. Accepted for publication 16 Feb 2024. Published online 25 Mar 2024.
This work was supported by the Excellent Youth Foundation of Henan Scientific Committee of China (212300410094), the Agricultural Science and Technology Innovation Program (ASTIP) (CAAS-ASTIP-2023-ZFRI), and the Special Fund of Henan Province for Agro-scientific Research in the Public Interest (no. 201300110500).
The authors declare that the data supporting the study findings are presented in the article and supplemental information files are available from the corresponding author upon request.
H.W. and A.L. contributed equally to this work.
W.Z., Z.W., and G.L. are the corresponding authors. E-mail: wangzhiqiang@caas.cn, zengwenfang@caas.cn, and liguohuai@mail.hzau.edu.cn.

fruit; however, in the softened fruit, there is little adhesion and a large intercellular gap (Ghiani et al. 2011). The flesh of softened apples (*Malus domestica*) showed a disrupted cell wall structure and reduced intercellular adhesion (Billy et al. 2008; Segonne et al. 2014). Using scanning electron microscopy to analyze the microstructure of fruit flesh, researchers found that mealy-textured apple fruits had dry granular structures with decreased intercellular adhesion (Brummell et al. 2004b; Li et al. 2020). Using transmission electron microscopy, it was also found that the middle lamella is dissolved in most mealy fruits (Ben-Arie et al. 1979). Homogalacturonan (HG) pectin is considered to play a major role in intercellular adhesion. The side chains of pectin, HG and rhamnogalacturonan I, interact with cellulose and are assumed to play a role in the mechanical characteristics of the cell wall (Lahaye et al. 2018). In HG, methylesterification of the C-6 carboxyl group of the galacturonic acid (GalA) residues contributes to the preservation of the integrity of the cell wall (Kinnaert et al. 2017). According to Li et al. (2020), apples have a high level of HG methylation throughout their immature stage; however, it significant decreases after mealiness.

Genes related to cell wall metabolism are closely associated with the process of fruit softening. In tomatoes (*Solanum lycopersicum*), inhibition of *SlPL* expression significantly increases fruit firmness at ripening (Uluisik et al. 2016; Wang et al. 2019). Studies of cell wall metabolism in Rosaceae fruits have mainly focused on PG and pectate lyase (PL) enzymes (Atkinson et al. 2012; García-Gago et al. 2009; Zhang et al. 2022). In strawberry (*Fragaria ×ananassa*), suppression of *FaPG1*, *FaplC*, or *FaβGal4* expression resulted in increased fruit firmness (García-Gago et al. 2009; Paniagua et al. 2014; Quesada et al. 2009; Youssef et al. 2013). Similarly, in apples, suppression of *MdPG1* expression also increased fruit firmness (Atkinson et al. 2012). Cell wall metabolic enzymes expressed early during fruit ripening can also have an impact on fruit ripening and softening. Reducing the expression of genes encoding pectin acetylesterase and cellulose synthase may accelerate fruit softening (Huang et al. 2017).

Changes in the cell wall structure are closely related to the metabolism of its constituents. The primary component that keeps the structure of pectin intact is HG, which comprises the linear chain of α-1,4-galacturonic acid (Mohnen 2008). Pectin methylesterase demethylates the GalA residues in HG pectins, whereas PG and PL cleave the main chain (Wormit and Usadel, 2018). Additionally, α-arabinofuranosidase and β-galactanase, respectively, remove the side chains of pectin and galactose. The catabolism of rhamnogalacturonan II pectin has been rarely reported (Nobile et al. 2011; Rui et al. 2017; Smith et al. 2002). Xyloglucan endotransglycosylase (XET) and xyloglucan hydrolase (XTH) are involved in the structural remodeling of xyloglucan in hemicellulose and in transferring glycosyl groups between two xyloglucan molecules (Anderson and Kieber 2020; Johnston et al. 2013; Shinohara et al. 2017). Other enzymes associated with hemicellulose modification and depolymerization include endo-1,4-β-glucanase, endo-β-mannanase, endo-xylosidase, and xylanase. In addition to the aforementioned enzymes, a large number of structural proteins, such as EXP and arabinogalactan proteins (AGPs), are also involved in cell wall metabolism (Brummell 2006; Goulao and Oliveira 2008; Wang and Seymour 2022). In addition, some cell wall-modifying proteins and transcription factors, such as trichome birefringence-like proteins (cell wall polysaccharide acetylation proteins) and lateral organ boundaries domain proteins (side organ boundary proteins), also regulate cell wall degradation and fruit softening (Shi et al. 2021).

The mealiness characteristic of fruits has been observed in peaches (Brummell et al. 2004a; Nilo-Poyanco et al. 2019), apples (Segonne et al. 2014), and pear (*Pyrus communis*) (Dong et al. 2018) during ripening or storage. Studies have shown that pectin is composed of (1→4)-linked α-d-GalA residues, and that pectin degradation and cell wall modification are associated with the mealy texture of fruits (Segonne et al. 2014). Although SH peaches are persistently not soft, we found that the expression of a freestone trait-related gene in SH peaches causes the fruits to soften and become mealy after ripening.

In this study, we explored the mechanism of fruit softening in peaches through the microstructural analysis of the flesh tissue of different SH-type cultivars using in situ immunolabeling of cell walls. We also compared the differences in cell wall composition among the cultivars. The expressions of 16 gene family members of cell wall metabolism-related genes were also analyzed to identify key genes associated with fruit softening in freestone-type SH peaches. Overall, this study provides a theoretical basis for the breeding and quality improvement of SH-type peaches.

## Materials and Methods

**Plant material and fruit sampling.** Four SH peach cultivars, including two clingstone cultivars that never soften (CP13 and CP9) and two freestone cultivars with mealy texture (CP14 and CPWJ2), were used during this study. Trees were grown at the Zhengzhou Fruit Research Institute, Chinese Academy of Agricultural Sciences, Zhengzhou, Henan, China. Fruits at the S4 I, S4 II, and S4 III stages were collected from different trees in 2020, as reported previously (Gabotti et al. 2015; Tonutti et al. 1997; Zeng et al. 2015). The mesocarp tissues of fruits were immediately frozen in liquid nitrogen and stored at −80 °C until needed for subsequent analyses (Pan et al. 2015).

**Evaluation of ethylene production and flesh firmness.** To measure ethylene production, each fruit sample was stored at 25 °C for 2 h in an airtight container with 0.5 mL of headspace, and the amount of ethylene produced was measured using the GC2010 gas chromatograph (GC2010; Shimadzu, Shanghai, China). Each sample was composed of three intact fruits and measured in triplicate. Flesh firmness was measured using a fruit pressure tester (GY-4-J; TOP, Zhejiang, China) (Zeng et al. 2015).

**Microstructural analysis of fruit flesh.** The mesocarp of peach fruits was cut into parallelepipeds of 4 mm × 3 mm × 2 mm and fixed in 2% (weight/volume) paraformaldehyde and 0.1% (weight/volume) glutaraldehyde in 0.1 M phosphate buffer (pH 7.2). The fixed tissues were washed with phosphate buffer, dehydrated using anhydrous ethanol series (10%, 20%, 30%, 40%, 50%, 60%, 70%, 80%, 90%, and 100%), and then dried in a critical point dryer (CPD030; Bal-Tec AG, Balzers, Liechtenstein) using liquid $CO_2$ as the transitional fluid. Each dried piece of mesocarp tissue was mounted on an anodized aluminum stub (IB-3; Eiko Co., Tokyo, Japan) using conducting silver glue. The tissue pieces were sputter-coated with a thin gold layer, and the surface morphology of each piece was observed using a scanning electron microscope (S-3400 N; Hitachi Co., Tokyo, Japan) at 15 kV (Li et al. 2020; Ng et al. 2013).

**Immunolabeling.** The fixed and ethanol-dehydrated sections were embedded in LR White resin (LR White resin; London Resin Company Ltd., London, UK) (Li et al. 2020), and then sliced into 1-μm-thick sections using a diamond knife and Leica UCT ultramicrotome (EM UC7; Leica Co., Wetzlar, Germany). The sections were mounted on poly-L-lysine-coated slides, dried overnight on a hot plate (45–50 °C), and immunolabeled with nonmethyl-esterified homogalacturonan labeling (LM19) and highly methyl-esterified homogalacturonan labeling (LM20) antibodies (PlantProbes, Leeds, UK) (Sutherland et al. 2004).

Immunolabeling was performed in a chamber created on the slide using a PAP pen (H-400; Vector Laboratories Co., Newark, CA, USA) by drawing a hydrophobic barrier around the sections. Briefly, sections were wetted for 10 min with phosphate-buffered saline containing 0.1% Tween 80 (PBS-T) (Millipore Sigma, St. Louis, MO, USA), and then incubated for 15 min in 0.1% bovine serum albumin (BSA-c; Aurion Biotech, Inc., Wageningen, Netherlands) dissolved in PBS-T to block nonspecific labeling. Subsequently, the sections were incubated overnight with primary antibodies (1:20 dilution in blocking buffer, volume/volume) in a humid chamber at 4 °C. After incubation, the slides were washed with PBS-T and incubated for 2 h with fluorescein isothiocyanate-conjugated goat antirat IgG secondary antibody (ZF-0315; ZSJQ-BIO Co., Beijing, China; 1:100 dilution in PBS-T, volume/volume) in the dark at room temperature. The immunolabeled sections were washed with 2 to 3 mL of PBS-T and coverslip-mounted on the slides using antifade agent solution (P0128S; Beyotime Co., Shanghai, China) (Li et al. 2020). Sections were viewed using a confocal laser scanning microscope (Fluoview FV1000 Espectral; Olympus Co., Tokyo, Japan). Images were taken at 40× magnification.

**Cell wall material extraction and fractionation.** Peach mesocarp tissue samples were ground in liquid nitrogen to obtain a uniform powder. Then, 5 g of each powdered sample was homogenized in 32 mL of 95% (volume/volume) ethanol and boiled for 30 min. The residue was separated and boiled twice (Li et al. 2020). After filtration, the insoluble residue was washed with 80 mL of acetone and partially dried by applying a mild vacuum. The yield of the obtained cell wall material (CWM) was calculated when fully dried. Then, 100 mg of CWM was sequentially extracted with cyclohexane-trans-1,2-diamine tetraacetic acid and sodium carbonate to obtain fractions enriched in water-soluble pectin (WSP), chelator-soluble pectin (CSP), and sodium carbonate-soluble pectin (SSP). Two hemicellulose-enriched fractions were obtained by extraction with 1 M and 4 M KOH (Li et al. 2019; Santiago-Doménech et al. 2008). Then, the insoluble residue was washed with double-distilled water until pH 7.0 and dried by applying a mild vacuum to obtain the cellulose.

**Transcriptome sequencing and quantitative reverse-transcription polymerase chain reaction.** Total RNA from peach fruit tissues was extracted using the TRIzol Reagent (TRIzol Reagent; Thermo Fisher Scientific, Waltham, MA, USA) and treated with RNase-free DNase (RNase-free DNase; Qiagen, Verogen Inc., San Diego, CA, USA). RNA-seq and bioinformatic analyses were conducted by Biomarker Technologies (Beijing, China). A total of 18 RNA-seq libraries (CP13 S4 I, S4 II, S4 III and CP14 S4 I, S4 II, S4 III) were constructed. Library construction was performed using the Illumina HiSEq 4000 (Illumina HiSEq 4000; Illumina, Inc., San Diego, CA, USA) sequencing platform. Clean reads were obtained by removing reads containing adapters, poly-N and low-quality reads from raw data with in-house Perlscripts (Niu et al. 2018). The quality score 20, quality score 30, and GC content values of the clean data were calculated. Reference genome and gene model annotation files were downloaded from the genome database for rosaceae (Jung et al. 2008). Relative transcript abundance was calculated based on the fragments per kilobase of exon model per million mapped fragments for biological replicates. HTSeq version 0.6.1 was used to count the read numbers mapped to each gene (Niu et al. 2018).

Gene-specific primers were designed using Premier 6.0 (Premier 6.0; Premier, Inc., Charlotte, NC, USA) (Supplemental Table 2). To perform the quantitative reverse-transcription polymerase chain reaction (qRT-PCR), total RNA was extracted from peach fruit tissues using the Total RNA Kit (Tiangen, Beijing, China) according to the manufacturer's instructions and assessed using the NanoDrop ND-1000 spectrophotometer (NanoDrop ND-1000; Thermo Fisher Scientific, Waltham, MA, USA). Then, cDNA was synthesized using the FastKing RT Kit (FastKing RT Kit; Tiangen, Beijing, China). The isolated cDNA was diluted to a concentration of 20 $ng \cdot \mu L^{-1}$ and used as a template for the qRT-PCR. Actin (Prupe.6G163400) was used as the internal reference gene (Tatsuki et al. 2013; You et al. 2021). Three replications per sample were performed.

**Identification of cell wall-related gene families.** The deduced amino acid sequences of peach genes were downloaded from the genome database for rosaceae (Jung et al. 2008), and those of Arabidopsis (*Arabidopsis thaliana*) genes were downloaded from the Arabidopsis information resource database (Swarbreck et al. 2008). All candidate sequences were submitted to the SMART database to verify the presence of conserved domains (Zhang et al. 2019). The proteins were detected using "Search Conserved Domains on a protein" at the National Center for Biotechnology Information website and classified according to the conserved domains specific to the gene family (Ma and Zhao 2010).

**Statistical analysis.** A one-way analysis of variance was performed using GraphPad Prism 9.0 software (GraphPad Prism 9.0; Graphpad Software, San Diego, CA, USA). Significant differences between groups were detected at $P < 0.05$. At least three biological replicates were used.

## Results

**Changes in peach fruit texture during ripening.** To distinguish SH clingstone and SH freestone peaches, the fruits of four peach cultivars, including two clingstone (CP13 and CP9) and two freestone (CP14 and CPWJ2) cultivars, were examined at the immature, mature, and mealy stages. At the immature stage, all four cultivars showed high fruit firmness (>30 N) and were clingstone-type. At maturity, the fruit firmness of all four cultivars decreased, but the firmness of CP13 and CP9 (>30 N) was higher than that of CP14 and CPWJ2 (>20 N). At the mealy stage, the 'CP14' and 'CPWJ2' fruits softened, and their firmness decreased to less than 10 N, whereas the firmness of 'CP13' and 'CP9' fruits remained higher than 25 N (Fig. 1B). During ripening, the single-fruit weight and soluble solid content of all four cultivars continued to increase, and the fruits released almost no ethylene. When fully ripened (at the mealy stage), the fruits of 'CP13' and 'CP9' were hard, whereas those of 'CP14' and 'CPWJ2' were freestone-type, soft, and mealy (Fig. 1A).

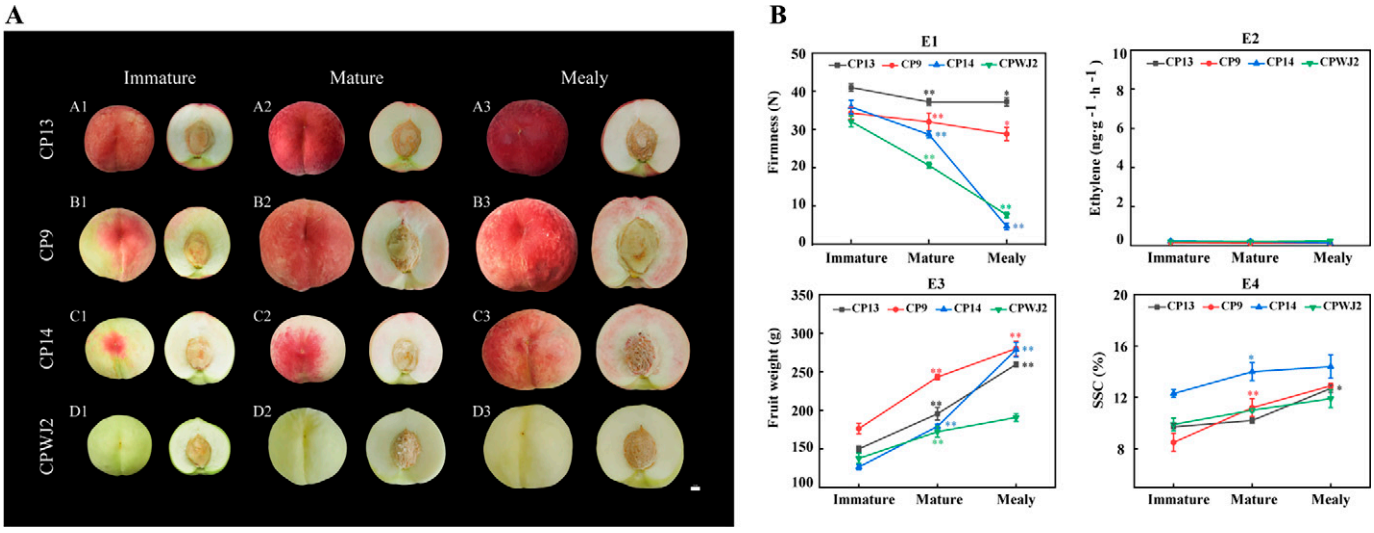


Fig. 1. Changes in the fruit traits of different peach cultivars during ripening. (**A**) Changes in the fruit traits of clingstone-type ('CP13' and 'CP9') and freestone-type ('CP14' and 'CPWJ2') fruits during ripening (A1–D3). S4 I (immature), S4 II (mature), and S4 III (mealy). 'Zhongtao 13' ('CP13'), 'Zhongtao 9' ('CP9'), 'Zhongtao 14' ('CP14'), and 'Zhongtao White Jade 2' ('CPWJ2'). (**B**) Changes in the fruit firmness (E1), ethylene production (E2), fruit weight (E3), and soluble solid content (SSC) (E4) of different peach cultivars during ripening (*$P < 0.05$; **$P < 0.01$). Error bars represent the *SE* of three independent biological replicates.

**Microstructural alterations in peach fruit texture.** Scanning electron microscopy was performed to examine the microstructure of the flesh tissues of each peach cultivar. At the immature stage, the fruits of all peach cultivars exhibited structurally intact cell walls. Parenchyma cells in the fractured surface were regularly arranged and showed minimal separation from adjacent cells (Fig. 2, A1, B1, C1, D1). At the mature stage, the flesh tissue of 'CP13' and 'CP9' fruits showed little change, with regularly arranged cells and minimal separation between adjacent cells (Fig. 2, A2, B2, A3, B3); 'CP14' showed larger intercellular spaces (Fig. 2, C2), and 'CPWJ2' showed the greatest change in the cell wall structure (Fig. 2, D2). Dried, intact, and separated, but

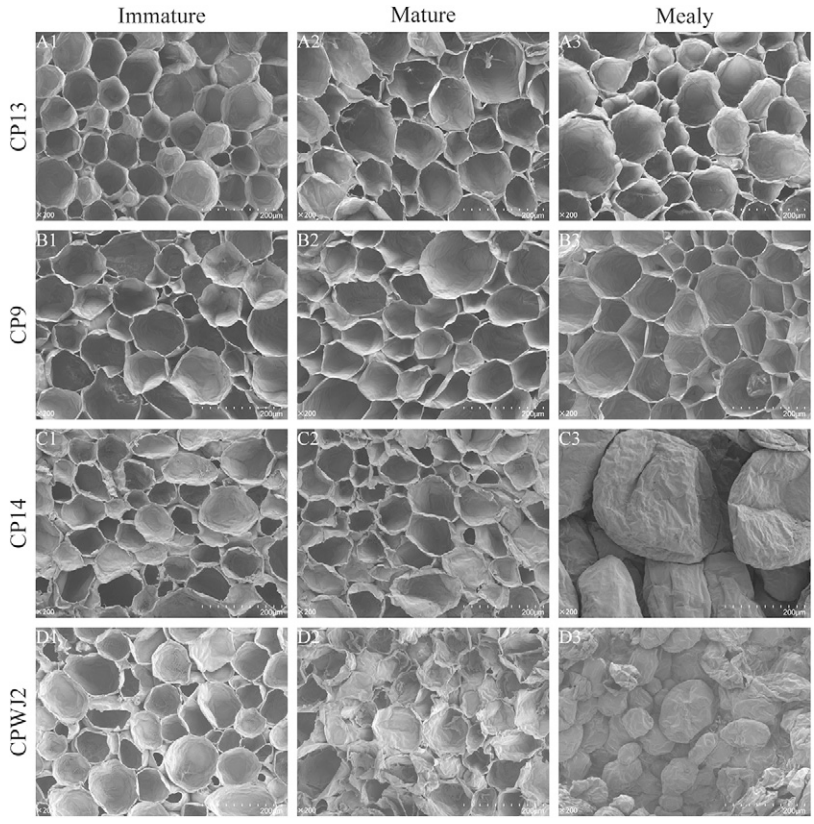


Fig. 2. Scanning electron microscopic images show tissue fracture patterns on the fruit surfaces of different peach cultivars during ripening. S4 I (immature), S4 II (mature), and S4 III (mealy). 'Zhongtao 13' ('CP13'), 'Zhongtao 9' ('CP9'), 'Zhongtao 14' ('CP14'), and 'Zhongtao White Jade 2' ('CPWJ2'). All images (A1–D3) were captured at 200× magnification (scale bars = 200 mm).

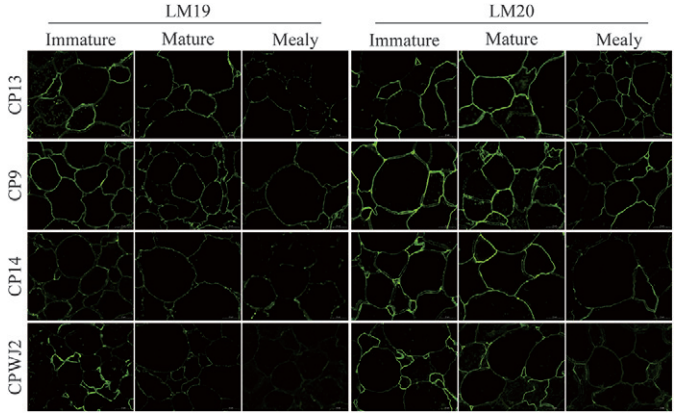


Fig. 3. Immunofluorescence of Homogalacturonan (HG) in the flesh tissues of different peach cultivars during ripening. Nonmethyl-esterified HG was labeled with nonmethyl-esterified homogalacturonan labeling (LM19) (A1–D3), and highly methyl-esterified HG was labeled with LM20 (E1–H3). S4 I (Immature), S4 II (Mature), and S4 III (Mealy). HG. 'Zhongtao 13' ('CP13'), 'Zhongtao 9' ('CP9'), 'Zhongtao 14' ('CP14'), and 'Zhongtao White Jade 2' ('CPWJ2'). Scale bars = 50 μm.

shriveled, cells were observed in the fractured surface of 'CP14' and 'CPWJ2' when the fruits were mealy (Fig. 2, C3, D3).

**Immunofluorescence labeling of HG in the cell wall.** To differentiate between methylated and nonmethylated pectins, in situ immunofluorescence monoclonal antibodies like LM19 and LM20 are typically used; LM19 identifies nonmethylated GalA residues, whereas LM20 binds to highly methylated pectin regions (Christiaens et al. 2016; Li et al. 2020; Ng et al. 2013). The fluorescence signal of LM19 was strong in the flesh tissues of 'CP13' and 'CP9' fruits at the immature stage. During the ripening process, the LM19 signal in the fleshy tissues of 'CP13' and 'CP9' diminished with time; however, at the same time points, it was stronger than the LM19 fluorescence signal in the flesh tissues of SH freestone peaches (Fig. 3, A1–A3, B1–B3). In the case of 'CP14' samples, the LM19 signal weakened even further during the ripening process; by the mealy stage (Fig. 3, C1–C3), only a faint fluorescence signal was visible. However, the LM19 signal in 'CPWJ2' samples was strong during the immature stage, but it was weakened during the mature and mealy stages. Compared with 'CP14' and 'CPWJ2' samples, the LM20 fluorescence signal in 'CP13' and 'CP9' samples was greater, and the levels of HG methylation in cells were lower during the mealy stage (Fig. 3, E1–H3).

**Fractions from CWM during peach ripening.** Changes in the polysaccharide fraction of the fruit cell wall varied among different peach cultivars. 'CP13' and 'CP9' showed a reduction in CWM during ripening, but the degree of reduction was not significant. In contrast, 'CP14' and 'CPWJ2' showed a smaller decrease in the CWM content at the immature and mature stages; however, at the mealy stage, the CWM content decreased significantly, especially that in 'CP14' (Fig. 4A, A1–A4). As the fruit ripened, nonmealy peaches 'CP13' and 'CP9' showed a significant decrease in the proportion of cellulose and a slight increase in the proportion of total pectin, indicating that cellulose is degraded into hemicellulose in the cell wall, and that the degradation of pectin is much lower than that of cellulose. Mealy peaches 'CP14' and 'CPWJ2' showed a significant decrease in the proportion of CSP and a significant increase in the proportion of SSP at the immature and mature stages while increasing significantly when the peaches became mealy. In 'CP14' and 'CPWJ2', the total WSP percentage increased, SSP percentage decreased, total pectin percentage decreased significantly, and cellulose percentage increased significantly (Fig. 4B, B1–B4). This indicated that pectin was degraded to a greater extent than

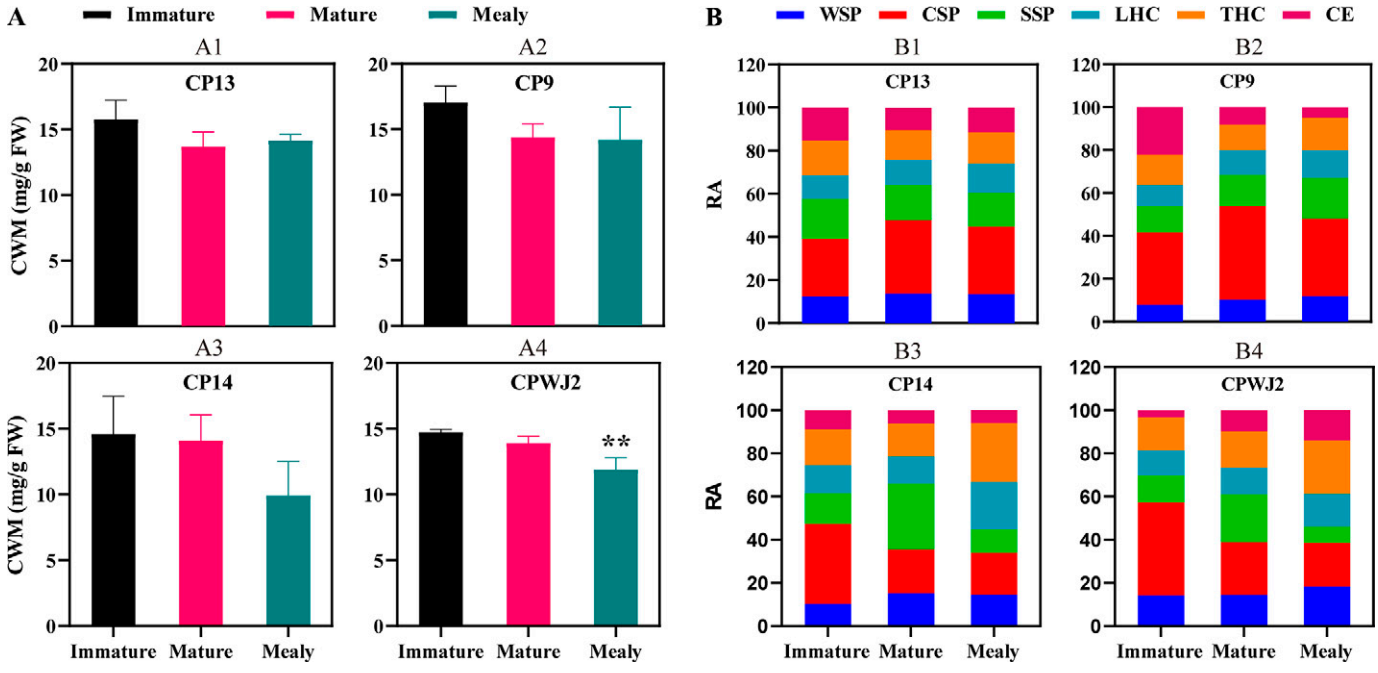


Fig. 4. Contents of cell wall material (CWM) fractions in peach fruit flesh. (**A**) Yield of CWM in the fruits of different peach cultivars during ripening (A1–A4) (**$P < 0.01$). (**B**) Percentage of galacturonic acid and cellulose in the CWM of different peach cultivars during ripening (B1–B4). S4 I (immature), S4 II (mature), and S4 III (mealy). Water-soluble pectin (WSP), chelator-soluble pectin (CSP), sodium carbonate-soluble pectin (SSP), loosely bonding hemicellulose (LHC), tightly bonding hemicellulose (THC), and cellulose (CE). 'Zhongtao 13' ('CP13'), 'Zhongtao 9' ('CP9'), 'Zhongtao 14' ('CP14'), and 'Zhongtao White Jade 2' ('CPWJ2'). Data represent the mean ± *SE* of three independent biological replicates.

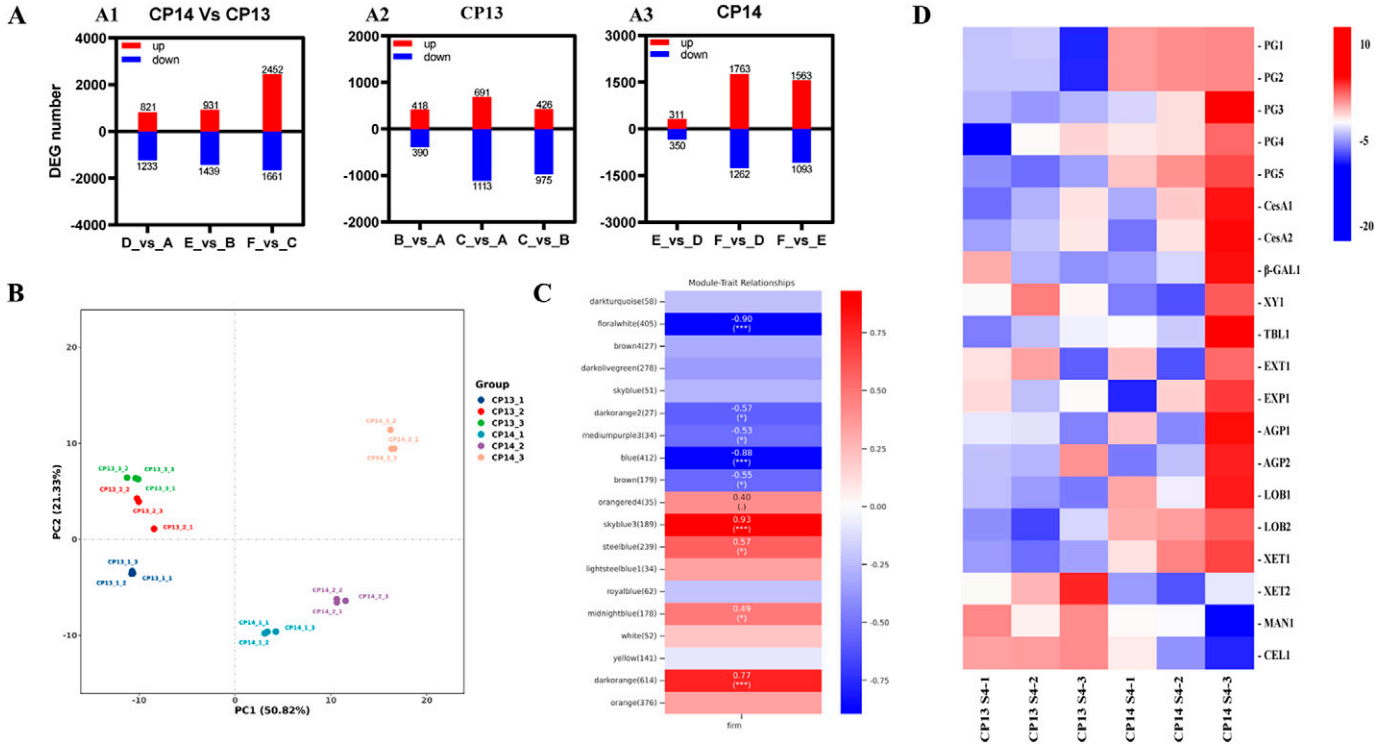


Fig. 5. Transcriptomic changes in peach fruits during ripening. (**A**) Numbers of differentially expressed genes (DEGs) identified in peach fruits during ripening (A1–A3). 'CP13' S4 I (A), 'CP13' S4 II (B), 'CP13' S4 III (C), 'CP14' S4 I (D), 'CP14' S4 II (E), and 'CP14' S4 III (F). (**B**) Principal component analysis (PCA) of DEGs using fragments per kilobase of exon model per million mapped fragments (FPKM) values as variables. CP13_1 ('CP13' S4 I), CP13_2 ('CP13' S4 II), CP13_3 ('CP13' S4 III), CP14_1 ('CP14' S4 I), CP14_2 ('CP14' S4 II), and CP14_3 ('CP14' S4 III). (**C**) Weighted gene coexpression network analysis (WGCNA) of firmness using FPKM values as variables. The color scale on the right represents the module–trait correlations ranging from −0.75 (blue) to +0.75 (red). (**D**) Heatmap display of genes showing strong correlation with fruit firmness. 'CP13' S4–1 ('CP13' S4 I), 'CP13' S4–2 ('CP13' S4 II), 'CP13' S4–3 ('CP13' S4 III), 'CP14' S4–1 ('CP14' S4 I), 'CP14' S4–2 ('CP14' S4 II), and 'CP14' S4–3 ('CP14' S4 III). 'Zhongtao 13' ('CP13') and 'Zhongtao 14' ('CP14'). S4 I (immature), S4 II (mature), and S4 III (mealy).

cellulose in the mealy peaches. In general, the degradation of CWM in SH clingstone peaches was less than that in SH freestone peaches. Additionally, during fruit ripening, the degradation of pectin was lower than that of cellulose in SH clingstone peaches, but greater than that of cellulose in SH freestone mealy peaches.

The CSP and SSP contents were significantly negatively correlated with the mealy texture, whereas CSP was significantly positively correlated with firmness and negatively correlated with CWM. This suggested that the degradation of CSP and SSP in the two types of SH peaches showed a strong correlation with the mealy texture, and that the changes in SSP content likely represent the degree of change in the mealy texture (Supplemental Fig. 1).

**Transcriptome analysis.** To reveal the mechanism responsible for the mealy texture of SH peaches, 18 RNA-seq libraries were constructed from the samples of 'CP13' (SH clingstone-type; S4 I, S4 II, and S4 III, designated as A, B and C, respectively) and 'CP14' (SH freestone-type; S4 I, S4 II, and S4 III, designated as D, E and F, respectively). A total of 118.70 Gb clean reads, equivalent to a total of 25,058 mRNAs, were obtained from the samples. The mapping rate of reads from all 18 libraries was >92.6%, and the average quality score 30 of the reads was >91.1%. The RNA-seq data obtained from the three biological replicates of each sample was highly correlated ($R^2 > 0.93$; $P < 0.01$). Therefore, the accuracy and quality of the RNA-seq data were determined to be sufficient for subsequent analyses. A principal component analysis revealed that the fruit samples from SH clingstone and SH freestone were significantly different from each other; however, all three biological replicates of each sample grouped together. The S4–3 sample of 'CP14' clustered independently from the other periods (Fig. 5B), suggesting that 'CP14' S4–3 was significantly different from the other periods. The S4–1 and S4–2 samples of CP13 grouped with those of 'CP14'. The number of differentially expressed genes (DEGs) between 'CP13' and 'CP14' was the highest during S4–3. Among these genes, 2452 were upregulated and 1661 were downregulated (Fig. 5A, A1–A3). Additionally, 189 genes in the sky-blue module, 405 genes in the floral-white module, and 412 genes in the blue module were significantly positively linked with the firmness according to a weighted gene coexpression network analysis of genes with fragments per kilobase of exon model per million mapped fragments values larger than 1 (Fig. 5C). Members of 18 gene families related to cell wall metabolism were compared with the genes exhibiting a highly significant correlation with firmness (Supplemental Table 1). A highly significant correlation between firmness and cell wall metabolism was seen in 17 upregulated genes and three downregulated genes (Fig. 5D).

**Gene expression analysis using qRT-PCR.** The qRT-PCR results showed that *PG1*, *PG2*, *AGP1*, *AGP2*, *EXT1*, and *EXP1* were significantly highly expressed in both freestone-type SH peach cultivars, indicating that these genes are jointly involved in cell wall degradation of SH freestone peaches (Fig. 6). Therefore, these genes were considered important candidates promoting the mealiness trait of freestone SH peaches. In contrast, *XET2* was significantly highly expressed in SH clingstone (nonmealy) peaches. Thus, *XET2* was considered an important candidate

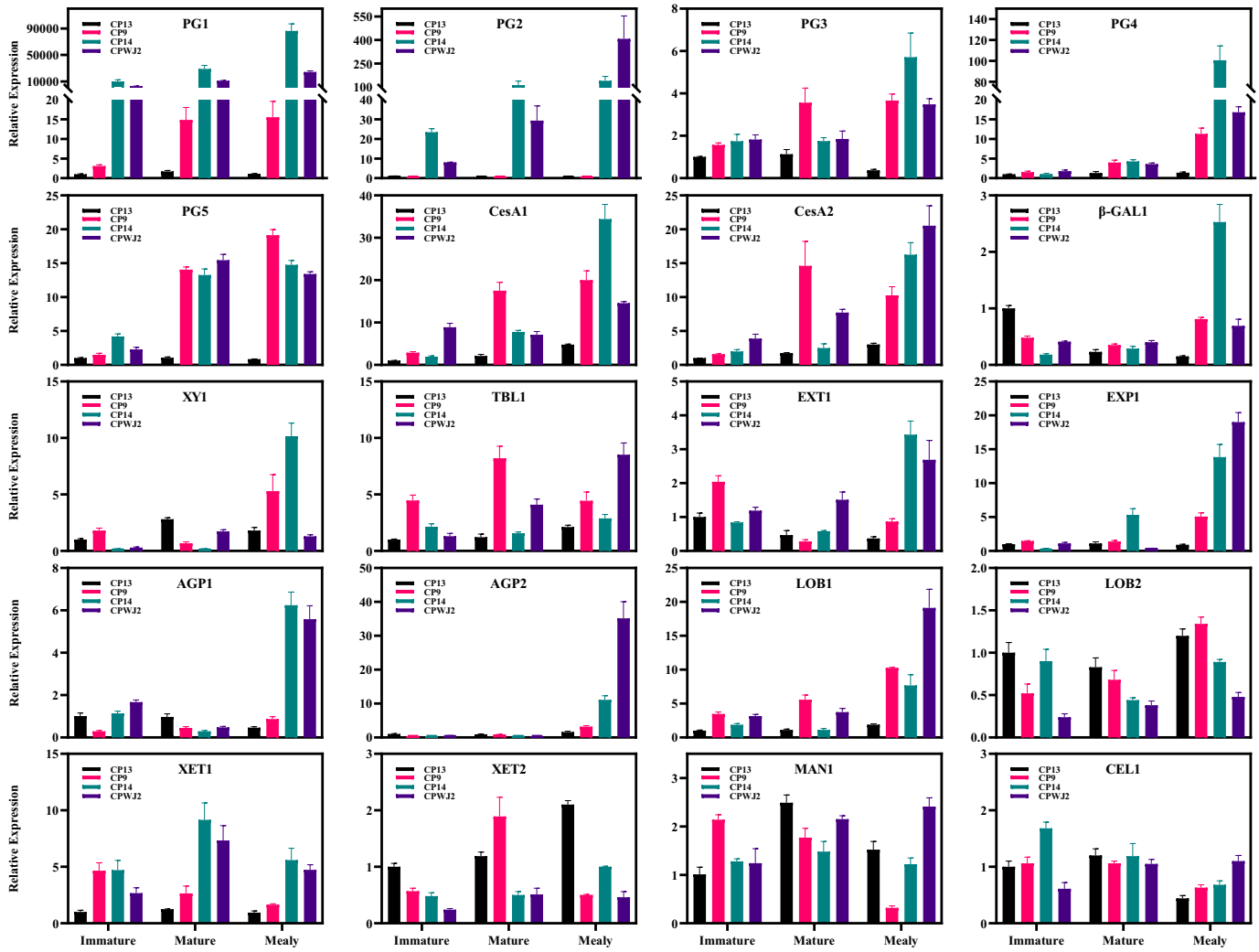


Fig. 6. Expression analysis of cell wall-related gene family members selected using weighted gene coexpression network analysis (WGCNA). 'Zhongtao 13' ('CP13'), 'Zhongtao 9' ('CP9'), 'Zhongtao 14' ('CP14'), and 'Zhongtao White Jade 2' ('CPWJ2'). Error bars represent the *SE* of three independent biological replicates.

that negatively regulates the genes responsible for the mealiness trait of SH freestone peaches.

Among all the selected genes, *PG1* showed the highest expression level, which was negatively correlated with fruit firmness and positively correlated with mealy texture. Fruit firmness was significantly negatively correlated with the *PG1*, *PG2*, *PG3*, *PG4*, *CesA1*, *CesA2*, *AGP1*, *AGP2*, and *LOB1* genes. Based on these results, *PG1*, *PG2*, *AGP1*, *AGP2*, *EXT1*, and *EXP1* were chosen as potential candidates for the mealiness attribute of freestone SH peaches. At the transcriptome level of 'CP13' and 'CP14', *XET2*, a negatively regulated gene, exhibited a highly significant negative connection with firmness; however, the fluorescence quantification results did not demonstrate a significant correlation (Supplemental Fig. 2). Therefore, the role of *XET2* in fruit ripening and its ability to regulate SH freestone fruit quality requires further investigation.

## Discussion

In our study, we found that clingstone-type SH peach fruits ('CP13' and 'CP9') have a very crispy flesh texture, but that freestone-type SH peach fruits ('CP14' and 'CPWJ2') ripen to a soft, mealy state. The microstructural analysis of SH peaches revealed that although mealy peaches had irregularly organized, dry, and shriveled cells with greater intercellular spaces, nonmealy peaches had densely packed, undamaged parenchyma cells. In a previous study, nonmealy apples showed regularly arranged parenchyma cells with minimal separation between adjacent cells (Li et al. 2020; Paniagua et al. 2014), similar to the results for 'CP13' and 'CP9' obtained during this study, whereas mealy apples showed dried, intact, and separated parenchyma cells (Li et al. 2020; Nobile et al. 2011; Segonne et al. 2014), similar to the microstructural observations of the mealy cultivars CP14 and CPWJ2.

Methylated pectins in nonmealy peaches, 'CP13' and 'CP9', showed little degradation during an immunofluorescence analysis, but nonmethylated pectins in mealy peaches, 'CP14' and 'CPWJ2', showed considerable degradation throughout the mealy stage. According to Li et al. (2020), methylated HG degraded slowly or was nearly nondegradable in nonmealy apples, consistent with the findings of the study. However, as apples reached the mealy stage, the amount of nonmethylated HG decreased (Ng et al. 2013).

The mealy and nonmealy textures of SH peaches were correlated with the changes in the pectin content, and the degradation of

pectin was the main cause of the reduced firmness of SH freestone peaches. Nonmealy peaches 'CP13' and 'CP9' showed little change in the proportion of each pectin component, consistent with the results of the study of the nonmealy apple cultivar Fuji (Li et al. 2020). The proportion of WSP considerably increased throughout fruit ripening in mealy peaches 'CP14' and 'CPWJ2', whereas the proportion of CSP first decreased and subsequently increased. The proportion of SSP exhibited an increasing trend, followed by a decreasing trend. A steady increase in the WSP content from the onset to the ripe and senescent stages was also observed in Golden Delicious apples (Gwanpua et al. 2016). The content of CSP decreased in slowly softening apples (Ng et al. 2013), whereas the content of CSP significantly increased and that of SSP sharply decreased in mealy apples (Li et al. 2020). These results are consistent with the greater firmness of 'CP14' and 'CPWJ2' fruits at the early stage and lower firmness at the late stage.

Reduced firmness and a mealy texture were the results of pectin breakdown in SH freestone peaches, which was positively connected with significantly high expressions of *PpPG1* and *PpPG2*. In apples, *MdPG1* is a candidate gene that impacts fruit texture and is associated with mealiness (Longhi et al. 2013). The main cause of the mealy texture was determined to be an abrupt breakdown of cell wall pectins associated with the imbalanced activity of many cell wall-modifying enzymes (Hayama et al. 2006). These results are similar to those of the current study in which high expression levels of *PpPG1* and *PpPG2* in 'CP14' and 'CPWJ2' resulted in mealy texture at ripening. This suggests that *PG* expression is a major factor that determines the texture of freestone and clingstone SH peaches.

*PpAGP1*, *PpAGP2*, and *PpEXP1* were also significantly highly expressed in SH freestone peaches, suggesting that these genes promote the mealy texture of SH freestone peaches. In apples, the effect of AGPs on fruit firmness is associated with different types of arabinoses in the cell wall (Lahaye et al. 2018), and the genes involved in the regulation of AGP activity may also be associated with fruit softening (Leszczuk et al. 2020). In the current study, the *PpAGP1* and *PpAGP2* family genes were significantly highly expressed in 'CP14' and 'CPWJ2' fruits at the mealy stage, suggesting that the expression of these genes is positively correlated with the mealy texture of SH freestone peaches. In tomato, the expression of *EXP1* was positively correlated with fruit softening (Hunter et al. 2021), similar to the expression of *PpEXP1* in this study. However, the content of EXP is reduced in mealy fruit (Obenland et al. 2003), and *EXP7* expression affects fruit softening (Brummell et al. 2004a, 2004b; Costa et al. 2008). Therefore, the role of EXP in the mealy texture of peach fruits requires further investigation.

## Conclusions

'CP14' and 'CPWJ2' are SH freestone mealy peaches that soften during ripening, lose adhesion between adjacent cells, and display separated, dried, and irregularly arranged cells. However, SH clingstone peaches are hard and have an intact cell wall structure. Our results suggest that six upregulated genes (*PpPG1*, *PpPG2*, *PpAGP1*, *PpAGP2*, *PpEXT1*, and *PpEXP1*) and one downregulated gene (*PpXET2*) are potentially involved in the development of the mealy texture of SH peaches. The molecular mechanisms regulating the softening and mealiness of SH peaches should be investigated further using the aforementioned genes as candidates.

## References Cited


Anderson CT, Kieber JJ. 2020. Dynamic construction, perception, and remodeling of plant cell walls. Annu Rev Plant Biol. 71(29):39–69. https://doi.org/10.1146/annurev-arplant-081519-035846.

Atkinson RG, Sutherland PW, Johnston SL, Gunaseelan K, Hallett IC, Mitra D, Brummell DA, Schröder R, Johnston JW, Schaffer RJ. 2012. Down-regulation of POLYGALACTURONASE1 alters firmness, tensile strength and water loss in apple (*Malus* × *domestica*) fruit. BMC Plant Biol. 12(1):129. https://doi.org/10.1186/1471-2229-12-129.

Ben-Arie R, Kislev N. 1979. Ultrastructural changes in the cell walls of ripening apple and pear fruit. Plant Physiol. 64(2):197–202. https://doi.org/10.1104/pp.64.2.197.

Billy L, Mehinagic E, Royer G, Renard CMGC, Arvisenet G, Prost C, Jourjon F. 2008. Relationship between texture and pectin composition of two apple cultivars during storage. Postharvest Biol Technol. 47(3):315–324. https://doi.org/10.1016/j.postharvbio.2007.07.011.

Brummell DA, Dal Cin V, Lurie S, Crisosto CH, Labavitch JM. 2004a. Cell wall metabolism during the development of chilling injury in cold-stored peach fruit: Association of mealiness with arrested disassembly of cell wall pectins. J Expt Bot. 55(405):2041–2052. https://doi.org/10.1093/jxb/erh228.

Brummell DA, Dal Cin V, Crisosto CH, Labavitch JM. 2004b. Cell wall metabolism during maturation, ripening and senescence of peach fruit. J Expt Bot. 55(405):2029–2039. https://doi.org/10.1093/jxb/erh227.

Brummell DA. 2006. Cell wall disassembly in ripening fruit. Funct Plant Biol. 33(2):103–119. https://doi.org/10.1071/FP05234.

Christiaens S, Van Buggenhout S, Houben K, Jamsazzadeh Kermani Z, Moelants KR, Ngouémazong ED, Van Loey A, Hendrickx ME. 2016. Process-structure-function relations of pectin in food. Crit Rev Food Sci Nutr. 56(6):1021–1042. https://doi.org/10.1080/10408398.2012.753029.

Costa F, Van de Weg WE, Stella S, Dondini L, Pratesi D, Musacchi S, Sansavini S. 2008. Map position and functional allelic diversity of *Md-Exp7*, a new putative expansin gene associated with fruit softening in apple (*Malus* × *domestica* Borkh.) and pear (*Pyrus communis*). Tree Genet Genomes. 4:575–586. https://doi.org/10.1007/s11295-008-0133-5.

Dong Y, Zhang S, Wang Y. 2018. Compositional changes in cell wall polyuronides and enzyme activities associated with melting/mealy textural property during ripening following long-term storage of 'Comice' and 'd'Anjou' pears. Postharvest Biol Technol. 135:131–140. https://doi.org/10.1016/j.postharvbio.2017.09.010.

Gabotti D, Negrini N, Morgutti S, Nocito FF, Cocucci M. 2015. Cinnamyl alcohol dehydrogenases in the mesocarp of ripening fruit of Prunus persica genotypes with different flesh characteristics: Changes in activity and protein and transcript levels. Physiol Plant. 154(3):329–348. https://doi.org/10.1111/ppl.12319.

García-Gago JA, Posé S, Muñoz-Blanco J, Quesada MA, Mercado JA. 2009. The polygalacturonase *FaPG1* gene plays a key role in strawberry fruit softening. Plant Signal Behav. 4(8):766–768. https://doi.org/10.1104/pp.109.138297.

Ghiani A, Onelli E, Aina R, Cocucci M, Citterio S. 2011. A comparative study of melting and non-melting flesh peach cultivars reveals that during fruit ripening endo-polygalacturonase (endo-PG) is mainly involved in pericarp textural changes, not in firmness reduction. J Expt Bot. 62(11):4043–4054. https://doi.org/10.1093/jxb/err109.

Goulao LF, Oliveira CM. 2008. Cell wall modifications during fruit ripening: When a fruit is not the fruit. Trends Food Sci Technol. 19:4–25. https://doi.org/10.1016/j.tifs.2007.07.002.

Gu C, Wang L, Wang W, Zhou H, Ma B, Zheng H, Fang T, Ogutu C, Vimolmangkang S, Han Y. 2016. Copy number variation of a gene cluster encoding endopolygalacturonase mediates flesh texture and

stone adhesion in peach. J Expt Bot. 67(6):1993–2005. https://doi.org/10.1093/jxb/erw021.
Gwanpua SG, Verlinden BE, Hertog MLATM, Nicolai BM, Hendrickx M, Geeraerd A. 2016. Slow softening of Kanzi apples (*Malus ×domestica* L.) is associated with preservation of pectin integrity in middle lamella. Food Chem. 211(15):883–891. https://doi.org/10.1016/j.foodchem.2016.05.138.
Haji T, Yaegaki H, Yamaguchi M. 2005. Inheritance and expression of fruit texture melting, non-melting and stony hard in peach. Scientia Hortic. 105(2):241–248. https://doi.org/10.1016/j.scienta.2005.01.017.
Hayama H, Tatsuki M, Ito A, Kashimura Y. 2006. Ethylene and fruit softening in the stony hard mutation in peach. Postharvest Biol Technol. 41(1):16–21. https://doi.org/10.1016/j.postharvbio.2006.03.006.
Huang B, Routaboul JM, Liu M, Deng W, Maza E, Mila I, Hu G, Zouine M, Frasse P, Vrebalov JT, Giovannoni JJ, Li Z, van der Rest B, Bouzayen M. 2017. Overexpression of the class D MADS-box gene *Sl-AGL11* impacts fleshy tissue differentiation and structure in tomato fruits. J Expt Bot. 68(17):4869–4884. https://doi.org/10.1093/jxb/erx303.
Hunter DA, Napier NJ, Erridge ZA, Saei A, Chen RKY, McKenzie MJ, O'Donoghue EM, Hunt M, Favre L, Lill RE, Brummell DA. 2021. Transcriptome responses of ripe cherry tomato fruit exposed to chilling and rewarming identify reversible and irreversible gene expression changes. Front Plant Sci. 12:685416. https://doi.org/10.3389/fpls.2021.685416.
Johnston SL, Prakash R, Chen NJ, Kumagai MH, Turano HM, Cooney JM, Atkinson RG, Paull RE, Cheetamun R, Bacic A, Brummell DA, Schröder R. 2013. An enzyme activity capable of endotransglycosylation of heteroxylan polysaccharides is present in plant primary cell walls. Planta. 237(1):173–187. https://doi.org/10.1007/s00425-012-1766-z.
Jung S, Staton M, Lee T, Blenda A, Svancara R, Abbott A, Main D. 2008. GDR (genome database for rosaceae): Integrated web-database for rosaceae genomics and genetics data. Nucleic Acids Res. 36:1034–1040. https://doi.org/10.1093/nar/gkm803.
Kinnaert C, Daugaard M, Nami F, Clausen MH. 2017. Chemical synthesis of oligosaccharides related to the cell walls of plants and algae. Chem Rev. 117(17):11337–11405. https://doi.org/10.1021/acs.chemrev.7b00162.
Lahaye M, Bouin C, Barbacci A, Le Gall S, Foucat L. 2018. Water and cell wall contributions to apple mechanical properties. Food Chem. 268:386–394. https://doi.org/10.1016/j.foodchem.2018.06.110.
Lester D. R, Sherman W. B, Atwell B. J. 1996. Endopolygalacturonase and the melting flesh (M) locus in peach. J Am Soc Horticultural Sci. 121(2):231–235. https://doi.org/10.21273/JASHS.121.2.231.
Leszczuk A, Kalaitzis P, Blazakis KN, Zdunek A. 2020. The role of arabinogalactan proteins (AGPs) in fruit ripening-a review. Hortic Res. 7(1):176. https://doi.org/10.1038/s41438-020-00397-8.
Li Q, Li J, Li H, Xu R, Yuan Y, Cao J. 2019. Physicochemical properties and functional bioactivities of different bonding state polysaccharides extracted from tomato fruit. Carbohydr Polym. 219:181–190. https://doi.org/10.1016/j.carbpol.2019.05.020.
Li Q, Xu R, Fang Q, Yuan Y, Cao J, Jiang W. 2020. Analyses of microstructure and cell wall polysaccharides of flesh tissues provide insights into cultivar difference in mealy patterns developed in apple fruit. Food Chem. 321:126707. https://doi.org/10.1016/j.foodchem.2020.126707.
Liverani A, Giovannini D, Brandi R. 2002. Increasing fruit quality of peaches and nectarines: The main goals of ISFFO (Italy). Acta Hortic. 592(592):507–514. https://doi.org/10.17660/ActaHortic.2002.592.68.
Longhi S, Hamblin MT, Trainotti L, Peace CP, Velasco R, Costa F. 2013. A candidate gene based approach validates Md-PG1 as the main responsible for a QTL impacting fruit texture in apple (*Malus* x *domestica* Borkh). BMC Plant Biol. 13:37. https://doi.org/10.1186/1471-2229-13-37.
Ma H, Zhao J. 2010. Genome-wide identification, classification, and expression analysis of the arabinogalactan protein gene family in rice (*Oryza sativa* L.). J Expt Bot. 61(10):2647–2668. https://doi.org/10.1093/jxb/erq104.
Mohnen D. 2008. Pectin structure and biosynthesis. Curr Opin Plant Biol. 11(3):266–277. https://doi.org/10.1016/j.pbi.2008.03.006.
Ng JK, Schröder R, Sutherland PW, Hallett IC, Hall MI, Prakash R, Smith BG, Melton LD, Johnston JW. 2013. Cell wall structures leading to cultivar differences in softening rates develop early during apple (*Malus* x *domestica*) fruit growth. BMC Plant Biol. 13:183. https://doi.org/10.1186/1471-2229-13-183.
Nilo-Poyanco R, Vizoso P, Sanhueza D, Balic I, Meneses C, Orellana A, Campos-Vargas R. 2019. A Prunus persica genome-wide RNA-seq approach uncovers major differences in the transcriptome among chilling injury sensitive and non-sensitive varieties. Physiol Plant. 166(3):772–793. https://doi.org/10.1111/ppl.12831.
Niu L, Pan L, Zeng W, Lu Z, Cui G, Fan M, Xu Q, Wang Z, Li G. 2018. Dynamic transcriptomes of resistant and susceptible peach lines after infestation by green peach aphids (*Myzus persicae* Sülzer) reveal defence responses controlled by the Rm3 locus. BMC Genomics. 19(1):846. https://doi.org/10.1186/s12864-018-5215-7.
Nobile PM, Wattebled F, Quecini V, Girardi CL, Lormeau M, Laurens F. 2011. Identification of a novel α-L-arabinofuranosidase gene associated with mealiness in apple. J Expt Bot. 62(12):4309–4321. https://doi.org/10.1093/jxb/err146.
Obenland DM, Crisosto CH, Rose JKC. 2003. Expansin protein levels decline with the development of mealiness in peaches. Postharvest Biol Technol. 29(1):11–18. https://doi.org/10.1016/S0925-5214(02)00245-4.
Paniagua C, Posé S, Morris VJ, Kirby AR, Quesada MA, Mercado JA. 2014. Fruit softening and pectin disassembly: An overview of nanostructural pectin modifications assessed by atomic force microscopy. Ann Bot. 114(6):1375–1383. https://doi.org/10.1093/aob/mcu149.
Pan L, Zeng W, Niu L, Lu Z, Liu H, Cui G, Zhu Y, Chu J, Li W, Fang W, Cai Z, Li G, Wang Z. 2015. PpYUC11, a strong candidate gene for the stony hard phenotype in peach (*Prunus persica* L. Batsch), participates in IAA biosynthesis during fruit ripening. J Expt Bot. 66(22):7031–7044. https://doi.org/10.1093/jxb/erv400.
Quesada MA, Blanco-Portales R, Posé S, García-Gago JA, Jiménez-Bermúdez S, Muñoz-Serrano A, Caballero JL, Pliego-Alfaro F, Mercado JA, Muñoz-Blanco J. 2009. Antisense down-regulation of the FaPG1 gene reveals an unexpected central role for polygalacturonase in strawberry fruit softening. Plant Physiol. 150(2):1022–1032. https://doi.org/10.1104/pp.109.138297.
Rui Y, Xiao C, Yi H, Kandemir B, Wang JZ, Puri VM, Anderson CT. 2017. POLYGALACTURONASE INVOLVED IN EXPANSION3 functions in seedling development, rosette growth, and stomatal dynamics in *Arabidopsis thaliana.* Plant Cell. 29(10):2413–2432. https://doi.org/10.1105/tpc.17.00568.
Sandefur P, Clark JR, Peace C. 2013. Peach texture. Hortic Rev. 41:241–302. https://doi.org/10.1002/9781118707418.ch06.
Santiago-Doménech N, Jiménez-Bemúdez S, Matas AJ, Rose JK, Muñoz-Blanco J, Mercado JA, Quesada MA. 2008. Antisense inhibition of a pectate lyase gene supports a role for pectin depolymerization in strawberry fruit softening. J Expt Bot. 59(10):2769–2779. https://doi.org/10.1093/jxb/ern142.
Segonne SM, Bruneau M, Celton JM, Gall SL, Francin-Allami M, Juchaux M, Laurens F, Orsel M, Renou JP. 2014. Multiscale investigation of mealiness in apple: An atypical role for a pectin methylesterase during fruit maturation. BMC Plant Biol. 14:375. https://doi.org/10.1186/s12870-014-0375-3.
Shinohara N, Sunagawa N, Tamura S, Yokoyama R, Ueda M, Igarashi K, Nishitani K. 2017. The plant cell-wall enzyme AtXTH3 catalyses covalent cross-linking between cellulose and cello-oligosaccharide. Sci Rep. 7:46099. https://doi.org/10.1038/srep46099.

Shi Y, Vrebalov J, Zheng H, Xu Y, Yin X, Liu W, Liu Z, Sorensen I, Su G, Ma Q, Evanich D, Rose JKC, Fei Z, Van Eck J, Thannhauser T, Chen K, Giovannoni JJ. 2021. A tomato LATERAL ORGAN BOUNDARIES transcription factor, SlLOB1, predominantly regulates cell wall and softening components of ripening. Proc Natl Acad Sci USA. 118(33):1–8. https://doi.org/10.1073/pnas.2102486118.

Smith DL, Abbott JA, Gross KC. 2002. Down-regulation of tomato beta-galactosidase 4 results in decreased fruit softening. Plant Physiol. 129(4):1755–1762. https://doi.org/10.1104/pp.011025.

Sutherland PW, Hallett IC, MacRae E, Fischer M, Redgwell RJ. 2004. Cytochemistry and immunolocalisation of polysaccharides and proteoglycans in the endosperm of green Arabica coffee beans. Protoplasma. 223(2-4):203–211. https://doi.org/10.1007/s00709-004-0036-8.

Swarbreck D, Wilks C, Lamesch P, Berardini TZ, Garcia-Hernandez M, Foerster H, Li D, Meyer T, Muller R, Ploetz L, Radenbaugh A, Singh S, Swing V, Tissier C, Zhang P, Huala E. 2008. The Arabidopsis Information Resource (TAIR): Gene structure and function annotation. Nucleic Acids Res. 36:1009–1014. https://doi.org/10.1093/nar/gkm965.

Tatsuki M, Nakajima N, Fujii H, Shimada T, Nakano M, Hayashi K, Hayama H, Yoshioka H, Nakamura Y. 2013. Increased levels of IAA are required for system 2 ethylene synthesis causing fruit softening in peach (*Prunus persica* L. batsch). J Expt Bot. 64(4):1049–1059. https://doi.org/10.1093/jxb/ers381.

Tonutti P, Bonghi C, Ruperti B, Tornielli GB, Ramina A. 1997. Ethylene evolution and 1-aminocyclopropane-1-carboxylate oxidase gene expression during early development and ripening of peach fruit. J Am Soc Hortic Sci. 122(5):642–647. https://doi.org/10.21273/JASHS.122.5.642.

Tucker G, Yin XR, Zhang AD, Wang MM, Zhu QG, Liu XF, Xie XL, Chen KS, Grierson D. 2017. Ethylene and fruit softening. Food Quality and Safety. 1:253–267. https://doi.org/10.1093/fqsafe/fyx024.

Uluisik S, Chapman NH, Smith R, Poole M, Adams G, Gillis RB, Besong TM, Sheldon J, Stiegelmeyer S, Perez L, Samsulrizal N, Wang D, Fisk ID, Yang N, Baxter C, Rickett D, Fray R, Blanco-Ulate B, Powell AL, Harding SE, Craigon J, Rose JK, Fich EA, Sun L, Domozych DS, Fraser PD, Tucker GA, Grierson D, Seymour GB. 2016. Genetic improvement of tomato by targeted control of fruit softening. Nat Biotechnol. 34(9):950–952. https://doi.org/10.1038/nbt.3602.

Van Der Heyden CR, Holford P, Richards GD. 1997. A new source of peach germplasm containing semi-freestone nonmelting flesh types. HortScience. 32(2):288–289. https://doi.org/10.21273/HORTSCI.32.2.288.

Wang D, Samsulrizal NH, Yan C, Allcock NS, Craigon J, Blanco-Ulate B, Ortega-Salazar I, Marcus SE, Bagheri HM, Perez Fons L, Fraser PD, Foster T, Fray R, Knox JP, Seymour GB. 2019. Characterization of CRISPR mutants targeting genes modulating pectin degradation in ripening tomato. Plant Physiol. 179(2):544–557. https://doi.org/10.1104/pp.18.01187.

Wang D, Seymour GB. 2022. Molecular and biochemical basis of softening in tomato. Mol Horticulture. 2:5. https://doi.org/10.1186/s43897-022-00026-z.

Wormit A, Usadel B. 2018. The multifaceted role of pectin methylesterase inhibitors (PMEIs). Int J Mol Sci. 19(10):2878. https://doi.org/10.3390/ijms19102878.

You S, Cao K, Chen C, Li Y, Wu J, Zhu G, Fang W, Wang X, Wang L. 2021. Selection and validation reference genes for qRT-PCR normalization in different cultivars during fruit ripening and softening of peach (*Prunus persica*). Sci Rep. 11(1):7302. https://doi.org/10.1038/s41598-021-86755-5.

Youssef SM, Amaya I, López-Aranda JM, Sesmero R, Valpuesta V, Casadoro G. 2013. Effect of simultaneous down-regulation of pectate lyase and endo-β-1,4-glucanase genes on strawberry fruit softening. Mol Breed. 31:313–322. https://doi.org/10.1007/s11032-012-9791-y.

Zeng W, Pan L, Liu H, Niu L, Lu Z, Cui G, Wang Z. 2015. Characterization of 1-aminocyclopropane-1-carboxylic acid synthase (ACS) genes during nectarine fruit development and ripening. Tree Genet Genomes. 11:18. https://doi.org/10.1007/s11295-015-0833-6.

Zeng W, Niu L, Wang Z, Wang X, Wang Y, Pan L, Lu Z, Cui G, Weng W, Wang M, Meng X, Wang Z. 2020. Application of an antibody chip for screening differentially expressed proteins during peach ripening and identification of a metabolon in the SAM cycle to generate a peach ethylene biosynthesis model. Hortic Res. 7:31. https://doi.org/10.1038/s41438-020-0249-9.

Zhang S, Ma M, Zhang H, Zhang S, Qian M, Zhang Z, Luo W, Fan J, Liu Z, Wang L. 2019. Genome-wide analysis of polygalacturonase gene family from pear genome and identification of the member involved in pear softening. BMC Plant Biol. 19(1):587. https://doi.org/10.1186/s12870-019-2168-1.

Zhang WW, Zhao SQ, Gu S, Cao XY, Zhang Y, Niu JF, Liu L, Li AR, Jia WS, Qi BX, Xing Y. 2022. FvWRKY48 binds to the pectate lyase FvPLA promoter to control fruit softening in *Fragaria vesca*. Plant Physiol. 189(2):1037–1049. https://doi.org/10.1093/plphys/kiac091.